

Scintillator-photomultiplier tube calibration and noise reduction for the Neutron Incident Calibration Experiment using cosmic rays

Edwin A. Bernardoni

In the search for WIMPs, silicon detectors, such as those used in DAMIC, need to be able to distinguish between signals caused by WIMPs and signals caused by background radiation. NICE (Neutron Incident Calibration Experiment) is an initiative to calibrate these detectors for background neutron events in the 100 keV to 500 keV range. A relation can be determined between neutron energy and ionization produced in the silicon detector by scattering a known incident neutron off of the silicon detector and measuring the ionization of the silicon as well as the energy of the scattered neutron. To measure the energy of the scattered neutron, several rings of scintillator-photomultiplier tube rods will be used. However, these must also be calibrated. An optimal coupling must also be determined for the rods. It is the primary purpose of this experiment to identify and eliminate noise produced in the scintillator-PMT setups as well as to determine which coupling is most suited for use in NICE. This determination will be based on the calculated time resolution and average number of photoelectrons produced.

I. INTRODUCTION

A. Motivation

Based on cosmological observations and simulations, the composition of the

universe can be broken down into three categories: approximately 5% of the universe is known matter, 25% is what is termed “dark matter,” and 70% of the universe is “dark energy.” The concept of dark matter was introduced to account for

gravitational effects that are not explained by visible matter (such as the higher than expected orbital velocities of stars in galaxies and clusters of galaxies). From these and other observations, dark matter is expected to have certain characteristics. It should be noted that for other theories, these expected characteristics differ. In the particular theory that relates to this experiment, dark matter particles are referred to as WIMPs (weakly interacting massive particles) and should behave in the following ways. First, dark matter should be a particle. Second, it should be cold and thus cluster. This is suggested by simulations of the formation of the universe. Dark matter should also be weakly interacting (have no charge and emit no light); otherwise it would have already been observed. Lastly, it should have mass to account for the gravitational effects mentioned previously.¹ All of these characteristics, however, also describe a neutron. For detectors such as those used by DAMIC, which measure electron and nuclear recoil, a low-mass dark matter particle and a neutron would look very similar (since both would produce nuclear recoil). Thus to differentiate between a neutron and a WIMP in such detectors, the ionization produced by neutron collisions with the detector must be identified. This is the purpose of NICE.

B. What is NICE?

NICE stands for Neutron Incident Calibration Experiment, which endeavors to implement the following setup to calibrate silicon detector for background neutrons in the range of 100 keV to 500 keV (see Figure 1). To begin the calibration, neutrons are

first produced by a beam of protons colliding with Lithium atoms. These neutrons then scatter off of the silicon detector producing a signal. The energies of these scattered neutrons are then measured using several rings of scintillating material connected to PMTs (photomultiplier tubes). Using the calculated incident and final energies of the neutrons, a relation of neutron energy to ionization of the silicon can be determined. Using this information, background neutrons in a particular energy range can be filtered out from the data. For this to work however, the scintillator-PMT setup itself must be calibrated.

C. Purpose

Before the scintillator-PMT setup can be used in NICE, a few questions have to be answered. First, is the setup sensitive enough to detect neutrons? The scintillator-PMT couplings must have a small enough time resolution to accurately determine the timing of the collision. This timing will be used later in the calibration to filter out background noise during the calibration as well as to determine where on the scintillator the particle hit. It is imperative then that the time resolution is small enough to allow for identification of various particles based on their TOF (time of flight) values. Second, how does the charge reading from the PMT relate to the actual energy of the neutron? The average number of photoelectrons produced in the photocathode of the PMT is used to find this. A larger photoelectron production rate is desired for more accurate readings of small energy particles (such as a scattered neutron with energy around 1 keV). It is the primary purpose of this experiment to identify and eliminate noise produced in the scintillator-PMT setups to a reasonable achievable amount as well as to determine which

coupling is more suited to be used in NICE based on the time resolution and the average number of photoelectrons produced.

D. Equipment

Four PMT-scintillator-PMT setups were considered in this experiment. Rods 1A-1B and 2A-2B used an acrylic cookie for the scintillator-PMT coupling, 4B-3B used optical grease, and 4A-3A used a silicon rubber gel cookie as the coupling. EJ-200 plastic scintillator was used for all rods with dimensions of 1 cm x 2 cm x 20 cm. Timing values were taken by using an EG&G Ortec 934 Constant-Fraction Discriminator to convert the pulse to a NIM logic signal which, using Model 622 LeCroy Coincidence units to set logical parameters and Phillips Scientific Model 794 Gate/Delay Generator units to shape and delay certain pulses, were then converted to ECL (emitter coupled logic) and recorded using a CC-USB CAMAC Controller. TDC (time-to-digital converter) values were taken in relation to a common stop. Charge produced by each event was recorded using an ADC (analog-to-digital converter) unit. In all setups, cosmic rays were used for the calibration.

II. TIME RESOLUTION

A. Method

To find the time resolution of a particular PMT-scintillator-PMT setup (see Figure 2), consider the histogram of $T_1 - T_2$ where T_1 is the time of PMT1 and T_2 is the time of PMT2. For the setup shown in Figure 3, this value should be almost constant with some error due to shallow angled cosmic rays.² From this, the FWHM (full width at half max) can be measured which is proportional to the time resolution.

A timing coincidence was required between PMT LYSO, PMT1, and PMT2.

B. Results

Chart 1 shows the calculated time resolution for each PMT-scintillator-PMT setup with all rods producing an FWHM of less than 1 ns (see Figure 4). Resolution was restricted primarily by the increments of the TDC values where the TDC value is a count of half-nanoseconds. A finer time resolution is possible with another rod added to reduce the number of shallow angle cosmic hits via a smaller solid angle. It was determined, however, that each coupling produced a sufficiently small time resolution to proceed to the next stage of testing.

III. NUMBER OF PHOTOELECTRONS

A. Method

To find the average number of photoelectrons produced by a PMT, consider a collection of charge values for two different PMTs correlated by event. For PMTs connected to the same scintillator, the plot of the ADC value of one PMT vs. the ADC value of the other PMT per event should follow a linear trend with slope determined by the different gains of the two PMTs. This is because for each event both PMTs receive the same amount of light from the scintillator with some error due to attenuation (which is negligible for the short rods used in this experiment). Now the histogram of one PMT's ADC values with restrictions set on the other PMT's corresponding ADC values (making the ADC value roughly constant) should resemble a Poisson distribution. The average number of hits is then given by \bar{n} in

$$P(n) = \frac{\bar{n}^n}{n!} e^{-\bar{n}}$$

\bar{n} is found by dividing the mean by the standard deviation and squaring. This value is then proportional to the number of photoelectrons.

For a closer correlation of charge readings, a setup such as that shown in Figure 3 is preferred. Due to noise produced by poor grounding of the amplifier, the setup shown in Figure 5 was used instead. This removed the need to split the signal produced by each PMT. Four PMT-scintillator-PMT setups were stacked with a PMT on the top and bottom rods giving timing data while the four PMTs on the middle rods gave ADC readings. A timing coincidence was required between the two PMTs recording timing data.

B. Results

Figure 6 shows the scatter plots of ADC vs. ADC for the four rods. The large spreads of Figures 6a and 6b mean that the standard deviation of each projected ADC slice is larger; thus the average number of photoelectrons is lower. On the other hand, Rod 3A-4A (Figure 6c) has the strongest correlation between the two ADC values and thus produces the most photoelectrons of the four rods. The gel cookie is then the optimal coupling for NICE.

IV. NOISE REDUCTION

Throughout this experiment, three main forms of noise were identified and eliminated when possible: poor grounding of

the amplifier modules, excessive internal PMT sparking, and clipping.

A. Amplifier

In the experiments with the cross-shaped arrangement (see Figure 3), it was necessary to split the signal from the PMT to get both a TDC and ADC value. To do this, an amplifier was used. Whenever the lights were switched on or off, the air conditioning turned on or off, or any moderately sized electrical device was used, however, a large oscillating signal was produced. When integrated, these phantom signals appear as lower ADC values (due to the positive and negative voltage oscillation) while having perfect time coincidence (since all initial TDC signals go through the same amplifier). It was later discovered that the amplifier was the source of these signals, possible as a result of different or poor grounding for the two outputs. Figures 7a and 7b show the difference in the ADC values between the crossed setup (using the amplifier) and the stacked setup (without any amplifier) for PMT2B.

B. Internal PMT Sparking

While analyzing the time resolution of the 3A-4A rod, excessive saturation of the ADC values from PMT3A were observed. The value read from the ADC is a 10-bit value, thus any value greater than 1024 is instead saved as the maximum value and called “saturated.” These saturated values and the corresponding values from PMT4A came in excess of 30 ns earlier than expected for a clean distribution (see Figure 8). Using an oscilloscope, it was discovered that PMT3A would occasionally produce a

large pulse greater than 3 volts at its peak as shown in Figure 9. The pulse proved large enough to saturate the amplifier and produce noise in PMT4A causing the pulse to be recorded as an event. Introducing a timing cut on the difference of the TDC values eliminated all of these signals.

C. Clipping

After the amplifier was removed, many of the excess small ADC valued pulses disappeared. However, a small but distinct collection of low ADC valued pulses still existed. As a result, there were two peaks in all of the ADC histograms where there should only be one. Each such pulse arrived perfectly in time, suggesting it was real. Increasing the voltage shifted both pulses; also suggesting these pulses were real. A low valued pulse in one PMT was always accompanied by either an equivalently low value in the other rod or a value close to those pulses residing in the larger peak (see Figure 10). All signs pointed to these pulses being real and in time with the actual cosmic rays. Eventually it was postulated that this behavior was a result of clipping (cosmic rays going through just the corner of a rod). A muon clipping both rods would read as a pair of low ADC values while a muon clipping one rod and hitting the other rod all the way through would read as a low and a high ADC value (Figure 11). The 2-to-1 ratio of the width to thickness of the rods made the effect more evident. A setup using a stack of four rods, each reading a TDC and ADC value, was used to verify this hypothesis (Figure 12). Preliminary data suggests that this is the case. For the actual NICE setup, the single point collision nature of the low neutrons with the scintillator eliminates this problem.

V. CONCLUSION

With the combination of all three noise reductions found and implemented in this experiment, the TDC and ADC data became much cleaner. Figure 13 shows a comparison of ADC vs. TDC before and after all three noise reductions for PMT3A. The change is dramatic, and the muons clearly identifiable from graphs such as in Figure 7b. The PMTs can now be further calibrated in future experiments with more confidence in the accuracy of the data received. The time resolution of all three couplings is sufficiently small for their desired purpose. Rod 3A-4A with the gel cookie coupling produces the most photoelectrons on average and is thus the desired coupling to using in NICE.

VI. ACKNOWLEDGMENTS

This work was supported in part by the U.S. Department of Energy, Office of Science, Office of Workforce Development for Teachers and Scientists (WDTS) under the Science Undergraduate Laboratory Internship (SULI) Program.

Mentorship by Gaston Gutierrez is gratefully acknowledged whose instruction made this possible. Support by Federico Izraelevitch is also gratefully acknowledged who allowed me to be associated with his larger project. Acknowledgement is made to Leonel Villanueva, a savant of cable attachments.

REFERENCES

- [1] James. Lochner, "The Hidden Lives of Galaxies," *Imagine the Universe!* 11 Aug 2005.
<http://imagine.gsfc.nasa.gov/docs/teachers/galaxies/imagine/titlepage.html> (31 July 2012).

- [2] Sumanta Pal and Vivek Singh, Measuring the energy spectrum of neutrons from a ^{252}Cf source using the time-of-flight techniques and a liquid scintillator with pulse shape discrimination property. (INO Graduate School, Tata Institute of Fundamental Research, Mumbai, India), pp. 2-3.

FIGURES

(Graphs produced by Wolfram's Mathematica)

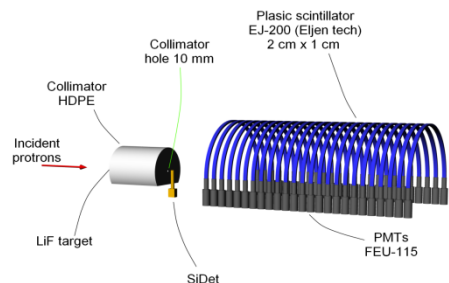


FIG. 1. Setup for NICE. Incident protons collide with the Lithium atoms in the LiF target producing Beryllium and neutrons. The incident neutrons then scatter off of the silicon detector producing a signal. The moment of the scattered neutron is the calculated from the measurements of the scintillator-PMT rings.

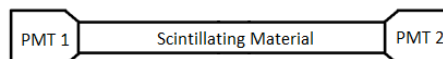


FIG. 2 Rods used for the calibration. The picture is of rod 2B-2A. The notation 2B-2A indicates that PMT1 corresponds to PMT1B and PMT2 corresponds to PMT2A.

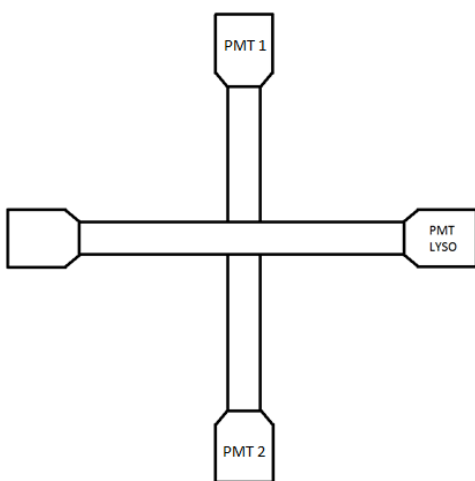


FIG. 3. Top view of the cross setup used for the calculation of the time resolution. The coincidence required between all three PMTs allows the system to only record events that occur in the center of both rods. This allows for more constant time values. Such a setup also decreases dark current triggers, as a miss-fire in all three rods is extremely unlikely.

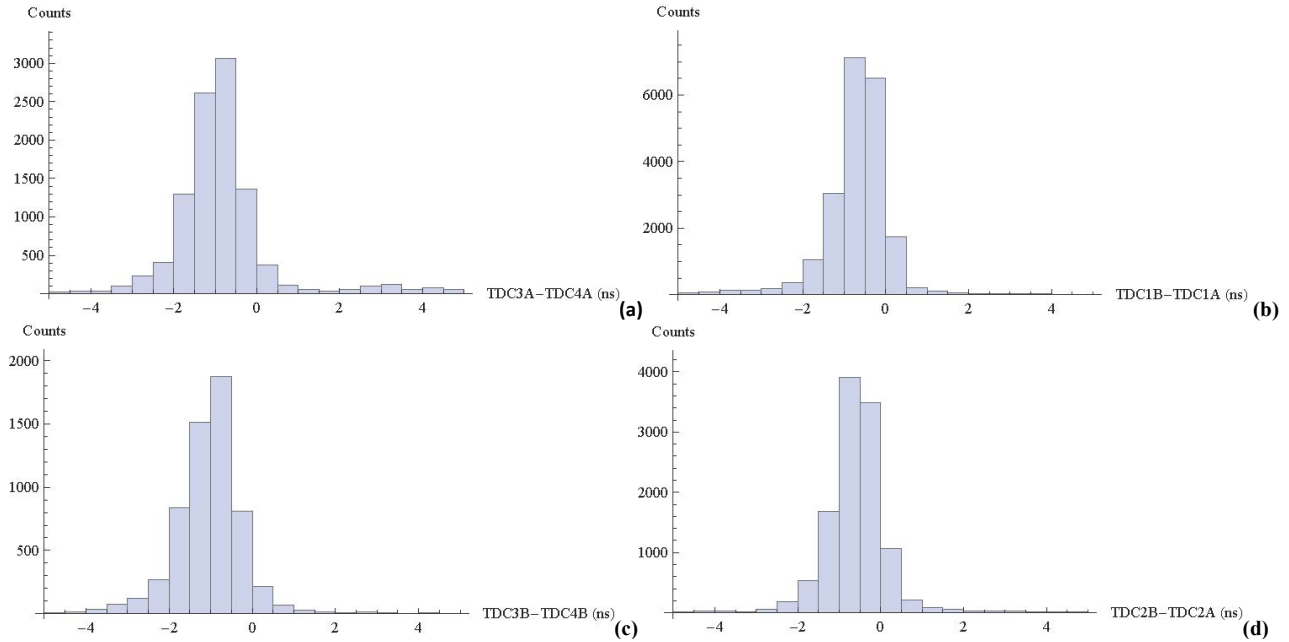


FIG. 4. (a)-(d) shows a sample histogram for each rod. The FWHM was found using these graphs and used to calculate the Time Resolution (See Chart 1). Bin size of 0.5 ns was chosen due to TDC values provided by the CAMAC unit being recorded in 0.5 ns increments.

Chart 1				
Bottom Rod	Top PMT	Total Events	FWHM (ns)	Time Resolution (ns)
3A-4A	2B	14341	<1	0.3
1B-1A	2B	24704	<1	0.3
3B-4B	2B	8361	<1	0.3
2B-2A	3B	13311	<1	0.3

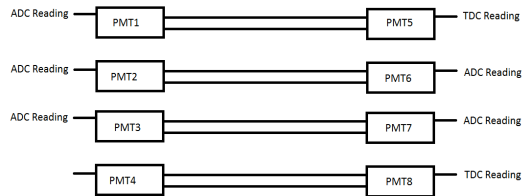


FIG. 5. Side view of the stacked setup used to find the average number of photoelectrons produced. A coincidence was required between PMT5 and PMT8, reducing the clipping effects of PMT2, PMT3, PMT6, and PMT7 observed in setups such as the crossed setup (See Figure 3). This setup also removes the need for an amplifier to split the signal while still allowing for two ADC values to be read from the same rod. This provides the stronger correlation necessary to find the average number of photoelectrons per PMT.

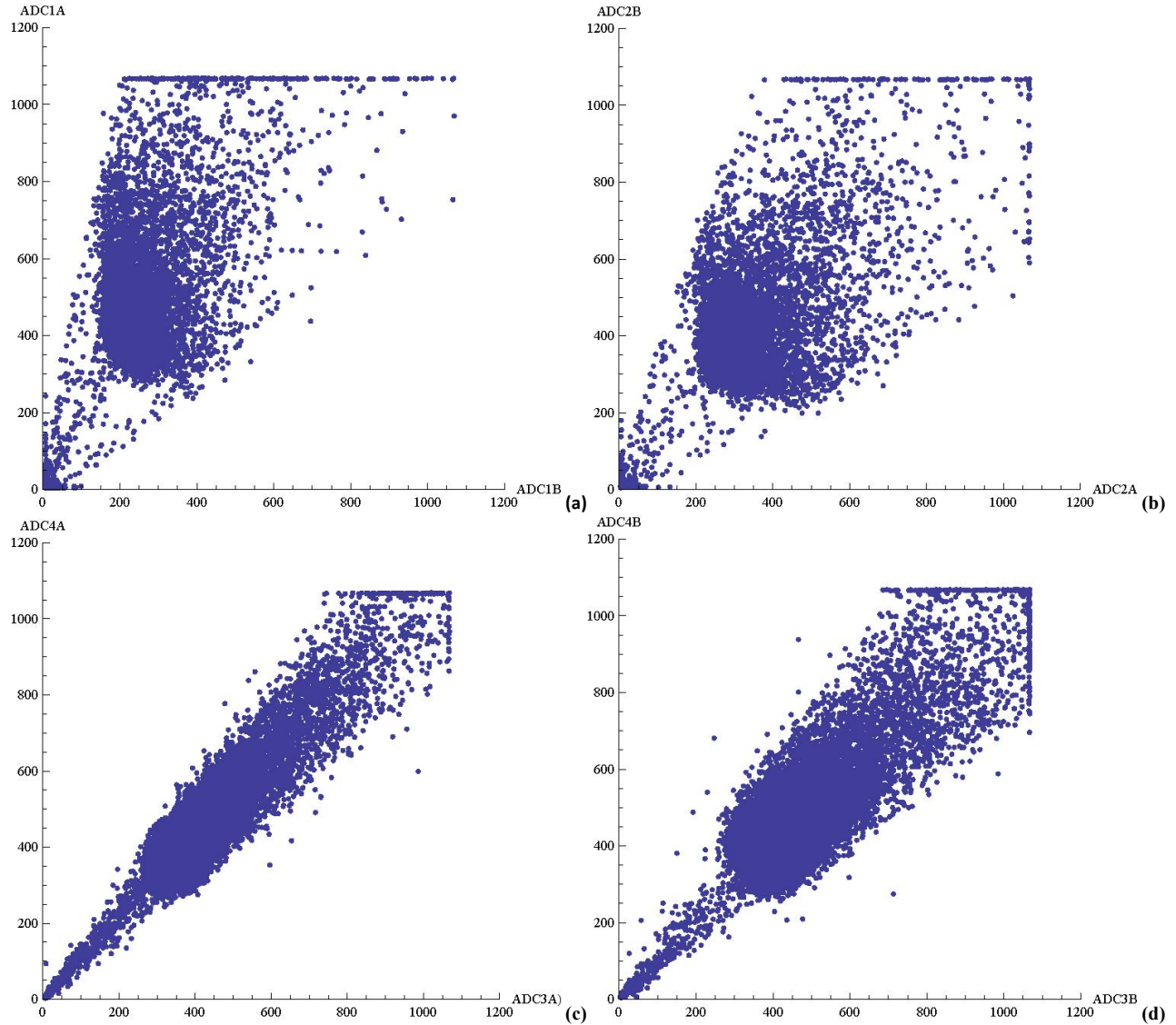


FIG. 6. (a)-(d) shows a sample scatterplot of ADC vs. ADC for each rod. The much tighter correlation (and thus lower standard deviation) of (c) means that rod 4A-3A produces more photoelectrons on average than the other rods. From these graphs alone, it is clear that the gel cookie is the optimal coupling for NICE.

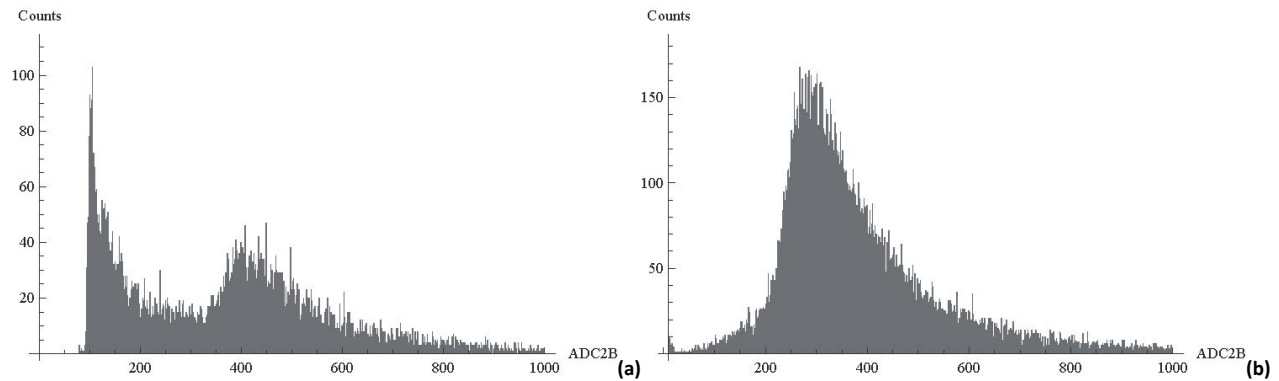


FIG. 7. (a) Histogram of the ADC values from PMT2B with the crossed setup (with an amplifier). Two peaks present: the low ADC valued peak

produced by amplifier noise and clipping effects, and the higher ADC valued peak consisting of the expected muon signal distribution. (b) Histogram of the ADC values from PMT2B with the stacked setup (no amplifier). Noise from the amplifier and clipping effects are completely removed with only the desired muon peak remaining.

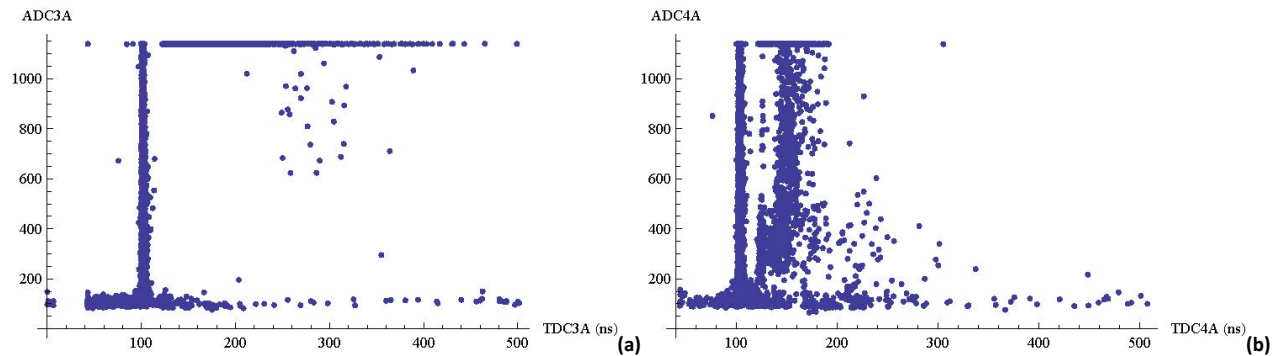


FIG. 8. (a) Scatterplot of the ADC vs. TDC values for PMT3A using the crossed setup (See Figure 3). A large spread of saturated ADC values occur at times greater than the 100ns bar produced by the muons. (b) Scatterplot of the ADC vs. TDC values for PMT4A using the crossed setup. A spread of various ADC values occur at times greater than the 100ns bar produced by the muons. Each of these data points correspond to a saturated value in PMT3A

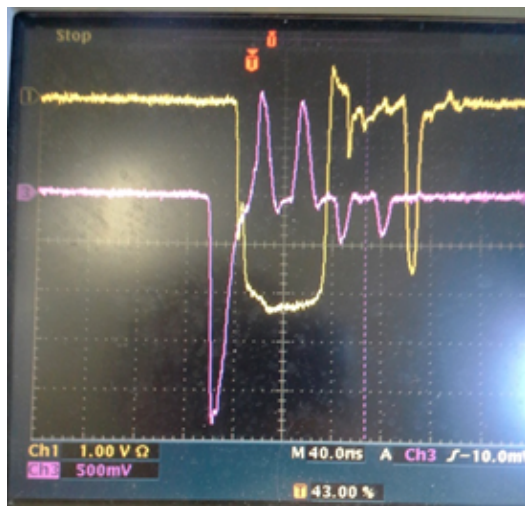


FIG. 9. Picture of the oscilloscope showing the large pulses produced by internal sparking of PMT3A. The pink pulse is the reading straight from the PMT while the yellow pulse is the corresponding signal from the amplifier (which is saturated).

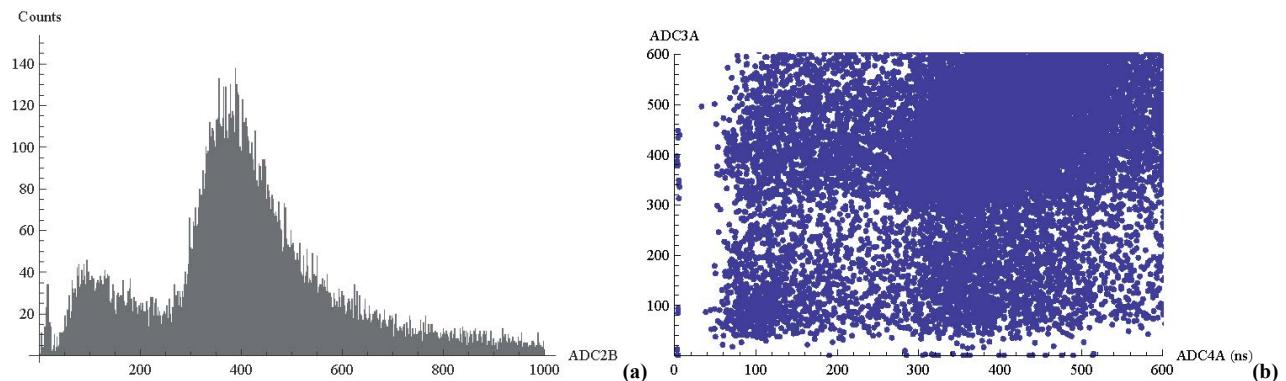


FIG. 10. (a) Histogram of the ADC values from PMT2B. Two peaks exist in the graphs where there should be one. The low valued ADC peak was

produced by clipping while the larger valued peak was produced by straight on collisions (See Figure 11). (b) Scatterplot of the ADC values from PMT3A vs. the corresponding ADC values from PMT4A. Four distinctive groupings appear in the plot: where both ADC values are around 400, both ADC values around 100, One ADC value is around 100 while the other is around 400, and vice versa. This grouping is due to the possible clipping effects (See Figure 11).

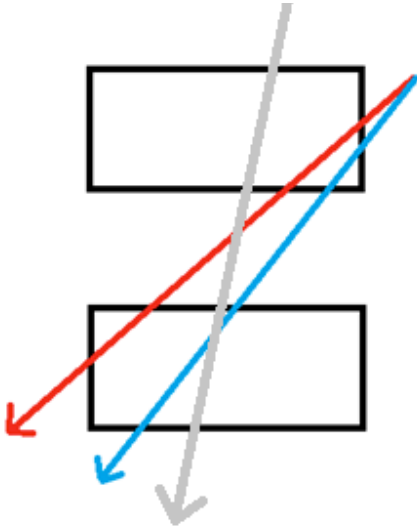


FIG. 11. Sketch of a cross-section of a stacked rod setup with three possible muon paths drawn. The grey arrow demonstrates a muon event with no clipping effects. The blue arrow demonstrates a muon event with clipping in the top PMT but not the bottom PMT. The red arrow demonstrates a muon event with clipping in both PMTs. These possible paths reach represent a grouping in Figure 10b where a longer path through the scintillator produces a larger ADC value.

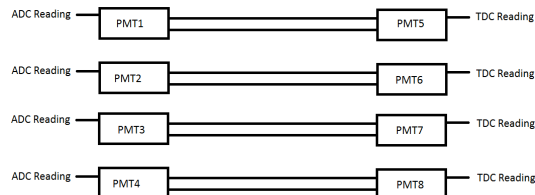


FIG. 12 Side view of the stacked setup used to test the clipping hypothesis. A coincidence was required between PMT5 and PMT8. For a perfectly aligned stack, the small valued ADC peak corresponding to clipping effects would mean that the two peaks in Figure 10a would be observed for PMT1 and PMT4 while only one peak would be observed for PMT2 and PMT3.

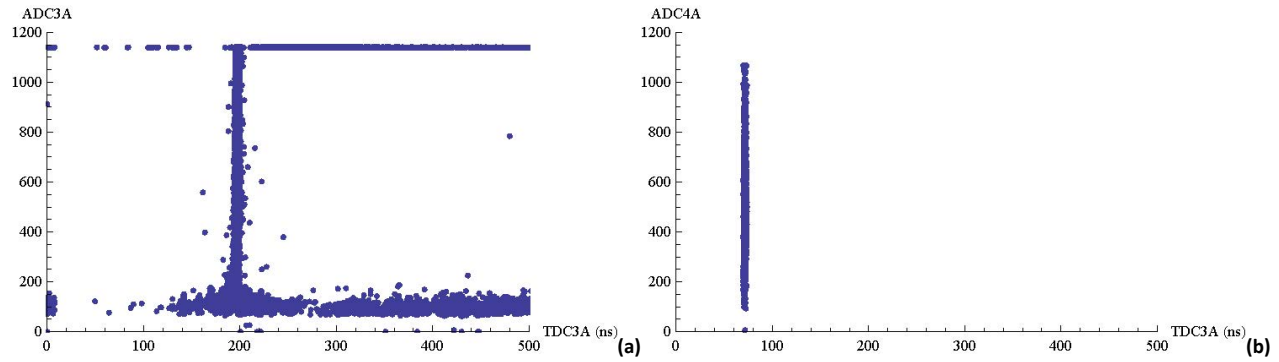


FIG. 13 (a) Scatterplot of ADC vs. TDC values for PMT3A with a crossed setup (See Figure 3). Amplifier noise, internal sparking of the PMT, and clipping effects were all present for this data set. (b) Scatterplot of ADC vs. TDC values for PMT3A with a stacked setup (See Figure 5). Amplifier noise and clipping effects were removed using the new setup and values from internal sparking were removed using timing constraints. The other PMTs show the same behavior without the need for timing constraint filters.